BIOORGANIC CHEMISTRY 9, 121–151 (1980)

The Solution Conformations of Gramicidin A and Its Analogs

S. V. SYCHEV, N. A. NEVSKAYA,[1] ST. JORDANOV, E. N. SHEPEL, A. I. MIROSHNIKOV, AND V. T. IVANOV

Shemyakin Institute of Bioorganic Chemistry, USSR Academy of Sciences, Moscow 117988, USSR

Received March 1, 1979

The conformational states in dioxane and ethanol of gramicidin A and of analogs varying in chain length and amino acid sequence have been studied. Infrared, CD, and polarization of fluorescence spectra of the peptides were measured, from which dimerization constants were determined and spectral characteristics of the monomeric and dimeric states obtained. Resonance splitting of the amide I ir band has been calculated for all gramicidin A models proposed earlier. Detailed comparison of the experimental and computed spectra showed that the four dimeric gramicidin species present in solution are predominantly antiparallel double $\uparrow\downarrow\pi\pi_{LD}$ helices in equilibrium with smaller amounts of head-to-head associated π_{LD} helices. The gramicidin A monomer was found to be a $\pi_{LD}^{4.4}$ helix in dioxane. For each conformational form the number of residues per turn and the helical sense were determined. The relationship between the amino acid sequence and the structure and stability of the dimer in the series of gramicidin A and its analogs is discussed. The above findings are rationalized in terms of the membrane channel properties of gramicidin A, in particular the conformational rearrangements occurring during the passage of metal ions through the channel and also the differences in conformation of the antibiotic in nonpolar solutions and in the membrane.

INTRODUCTION

Gramicidin A is a linear polypeptide antibiotic facilitating passive transmembrane transport of alkali metal ions and protons (*1*). It consists of 15 alternating L- and D-hydrophobic amino acid residues. Synthetic bilayers manifest discrete conductivity changes in the presence of very minute amounts of gramicidin A due to formation and breakdown of individual gramicidin A channels (*2*) made up of two polypeptide molecules (*3–6*).

Veatch *et al.* (*7*) found by thin-layer chromatography that there are four slowly interconverting gramicidin A dimeric species in solution, and these were isolated and characterized by CD, ir, and nmr spectroscopy and polarization of fluorescence (PF). The content of each of these forms in solution under equilibrium conditions was then determined (*8*).

The first possible model of a dimeric gramicidin A channel was proposed independently by Ramachandran and Chandrasekharan (*9*) and by Urry *et al.* (*10, 11*). In this model two gramicidin A molecules which are in a novel type of helical conformation aggregate in a head-to-head fashion (formyl end to formyl

[1] Institue of Protein Research, USSR Academy of Sciences, Pushchino, 142292, USSR.

0045-2068/80/010121-31$02.00/0

end), although other possibilities of double length dimer formation were not excluded. Urry termed this type of conformation a π_{LD} helix; the corresponding dimer we designate as a $\overrightarrow{\pi_{LD}}\,\overleftarrow{\pi_{LD}}$ helix. Urry proposed four types of such π_{LD} helices differing from each other in the number of residues per turn; of these the one best fitting a lipid membrane (30 Å thick) is the $\pi^{6.3}_{LD}$ helix (6.3 residues per turn), resulting in a pore diameter of 4 Å (*11*).

Veatch *et al.* (*7*) proposed another dimer model, a double helix wherein two peptide chains are coiled about a common axis. In contrast to the $\overrightarrow{\pi_{LD}}\,\overleftarrow{\pi_{LD}}$ dimer this double helix has no intermolecular hydrogen bonds, but some 28–30 intermolecular ones. The direction of the helical chains can be either parallel (⇈) or antiparallel (⇅). Of the family of double helices those with approximately six to seven residues per turn and internal diameter 3–5 Å possess a length of 30 Å (*7*). A common feature of the π_{LD} and double helices is the existence of a pore along the helical axis lined by oxygen atoms of the peptide groups, and orientation of all the side chains toward the solvent.

Lotz *et al.* (*12, 13*) have investigated the helical conformations of poly (γ-benzyl-LD-glutamate), which is regarded as a stereochemical model of gramicidin A. They showed that such a polymer can in fact exist both as π_{LD} helices and double helices, the latter being designated as $\pi\pi_{LD}$ helices. In Ref. (*13*) conformational calculations were carried out for poly(D–Ala–L–Ala). The atomic coordinates and the exact number of residues per turn for a number of $\pi\pi_{LD}$ and π_{LD} helices were determined.

In a study of the behavior of gramicidin A analogs with covalently bridged C termini or with charged groups on the N or C termini, Bamberg and co-workers (*14–16*) and Bradley *et al.* (*17*) favored $\overrightarrow{\pi_{LD}}\,\overleftarrow{\pi_{LD}}$ structures as the basic conducting conformations of gramicidin A. However, despite the numerous conjectures and indirect data, none of the proposed gramicidin A dimeric structures whether in solution or in the membrane, was favored.

In an attempt to obtain more definite knowledge of the state of gramicidin A in solution and in the membrane, we investigated further the conformational states of the antibiotic using also a number of synthetic analogs (*18*) differing from the parent compound in chain length, or in the nature of the amino acid residues.

	1	2	3	4	5	6	7	8	9	10	11	12	13	14	15
	L		L	D	L	D	L	D	L	D	L	D	L	D	L
	HCO–Val–Gly–Ala–Leu–Ala–Val–Val–Val–Trp–Leu–Trp–Leu–Trp–Leu–Trp–NH(CH$_2$)$_2$OH														
	Gramicidin A														
1	HCO–Val–Gly–Ala–Leu–Ala–Val–Val–Val–*Gly*–Trp–Leu–Trp–Leu–Trp–Leu–Trp–NH(CH$_2$)$_2$OH														
	D														
2	HCO–*Leu*–Val–Gly–Ala–Leu–Ala–Val–Val–Val–Trp–Leu–Trp–Leu–Trp–Leu–Trp–NH(CH$_2$)$_2$OH														
3	HCO–Val–Gly–*Val*–Leu–*Val*–*Leu*–Val–*Leu*–Trp–Leu–Trp–Leu–Trp–Leu–Trp–NH(CH$_2$)$_2$OH														
4	HCO–Val–Gly–Ala–Leu–Ala–Val———Trp–Leu–Trp–Leu–Trp–Leu–Trp–NH(CH$_2$)$_2$OH														
5	HCO–Val–Gly–Ala–Leu–Ala–Val–Val–Val———Trp–Leu–Trp–Leu–Trp–NH(CH$_2$)$_2$OH														
6	HCO–Val–Gly–Ala–Leu–Ala–Val–Val–Val———Trp–Leu–Trp–NH(CH$_2$)$_2$OH														
7	HCO–Val–Gly———–Val–Val–Trp–Leu–Trp–Leu–Trp–Leu–Trp–NH(CH$_2$)$_2$OH														
8	HCO–Val–Gly———–Trp–Leu–Trp–Leu–Trp–Leu–Trp–NH(CH$_2$)$_2$OH														

To achieve our objective we carried out a detailed comparison of the ir spectra of the gramicidin A conformational species with the spectra calculated for all the earlier proposed structural models. The theoretical part was based on a recently

developed method for calculating the resonance interactions of the amide vibrations (*19–21*) and on determinations of the atomic coordinates of the polypeptide backbone in the $\pi\pi_{LD}$ and π_{LD} helices (*13*).

The aggregation state of the analogs was studied preliminarily by CD and PF by a method similar to that carried out for gramicidin A, it being found that here too dimerization took place and that the solution consisted of a mixture of interconverting dimers. The equilibrium mixture of gramicidin A and its analogs was found to be more complicated than had been envisaged earlier, each of the four dimer species being in turn an equilibrium mixture of three different helical forms. Molar fractions and structural parameters were determined for all forms. The findings were of considerable consequence in obtaining a deeper insight into the possible state of a gramicidin A channel in the membrane.

EXPERIMENTAL

Materials. Synthetic gramicidin A (*18*) was recrystallized once from ethanol. Species 3[2] was obtained as described in Ref. (*7*). Ethanol and methanol were once distilled over sodium. Dioxane was carefully purified from traces of aromatic hydrocarbons by twice distilling a 1 : 10 dioxane : water mixture in a rectifying column of 30 theoretical plates and checking the absence of aromatic hydrocarbons by measuring the absorption in the 300- to 230-nm region.

Circular dichroism (CD). Spectra were recorded at room temperature on a Cary 60 spectrometer equipped with a Model 6001 CD attachment and on a Jobin Yvon Dichrograph III. Quartz cells of varying thickness from 0.001 to 5 cm were used; 0.01 cm and thinner cells were measured by the interference fringe method. The CD data were converted to dichroic differences per residue.

Infrared (ir). Spectra were recorded at ca. 35°C on a Perkin–Elmer 180 spectrophotometer at 2 cm^{-1} resolution, using 0.1–1 mm CaF_2 and 2.60 mm NaCl cells. The error in determining the molar absorption coefficient did not exceed 30 $M^{-1} \cdot cm^{-1}$ and the peak positions was less than ± 0.5 cm^{-1}.

Fluorescence. Measurements were carried out at 25°C in stoppered 1-cm quartz cells on a Hitachi MPF-3 spectrofluorimeter equipped with temperature control and polarization accessories. Excitation was at 290 nm and emission was monitored at 340 nm. The polarization was calculated as the intensity ratio of the perpendicular to the parallel components after correction for the efficiency of the emission monochromator grating.

Monitoring of equilibration. For determining the equilibration time the CD spectra of gramicidin A and of its analogs were measured at various periods following their solution. Conformational equilibrium of gramicidin A analogs becomes established in 24 hr after solution in ethanol and from 1–6 days,

[2] Here and in the following for simplicity the term "species" will refer to the gramicidin A species of Veatch *et al.* (*7*). Thus species 3 means gramicidin A species 3. However, the term refers to the structure rather than the substance and will be used also for denoting the corresponding structure in the analogs. Thus species 3 when referred to analog 2 means an analog 2 species corresponding to gramicidin A species 3.

depending upon the compound, after solution in dioxane. In the case of gramicidin A in dioxane equilibration occurs only after over 20 days, as found by Veatch and Blout (*8*). All the CD and ir spectra given here were obtained under equilibrium conditions.

METHODS AND RESULTS

Aggregation of Gramicidin A Analogs

The aggregation of gramicidin A analogs in dioxane and ethanol was studied by CD and PF techniques. The measurements were made over a maximum range of concentrations limited on the one hand by the optical density of the solution, and on the other, by the sensitivity of the instrument. Ordinarily this range was from 10^{-5} to $10^{-2}\,M$. In most cases changes in the CD curves were observed on passing from dilute to more concentrated solutions, owing to aggregation of the peptide.

The concentrational dependence of the dichroic absorption was analysed as follows. It was assumed that the change in absorption ($\Delta\epsilon'$) with increase in peptide concentration (c) is due to shift in the equilibrium:

$$A + A \rightleftarrows A_2,$$

characterized by the dimerization constant (K_{dim}),

$$K_{\text{dim}} = \frac{[A_2]}{[A]^2}. \qquad [1]$$

The value of K_{dim} is obtained from the equation for a second-order reversible reaction:

$$1 - \frac{c_1}{c_c} = 2\,K_{\text{dim}} \cdot c \left(\frac{c_1}{c}\right)^2, \qquad [2]$$

where $c = A + 2A_2$ is the overall concentration known from the experimental conditions and

$$\frac{c_1}{c} = \frac{\Delta\epsilon'_{\text{dim}} - \Delta\epsilon'_{\text{obs}}}{\Delta\epsilon'_{\text{dim}} - \Delta\epsilon'_{\text{mon}}}$$

is the molar fraction of the monomer.

Here the values $\Delta\epsilon'_{\text{dim}}$ and $\Delta\epsilon'_{\text{mon}}$ correspond to the values observed at high dilution or maximum concentration, respectively, when further dilution or higher concentration has no effect on the CD curve. When $\Delta\epsilon'_{\text{mon}}$ or $\Delta\epsilon'_{\text{dim}}$ cannot be accurately measured, their values are obtained by extrapolating $\Delta\epsilon'_{\text{obs}}$ vs $\log c$ to high and low concentration regions. After determination of K_{dim} the theoretical $\Delta\epsilon'$ vs $\log c$ curve is plotted according to Eq. [2], and the plot is compared with the experimental data. For the computation, $\Delta\epsilon'$ values at 228 nm were usually taken, as maximum dichroic absorption was observed at that wavelength. The value of K_{dim} was calculated in the same way also from the concentrational dependence of PF, but using the parameter $d = I_1/I_{\|}$.

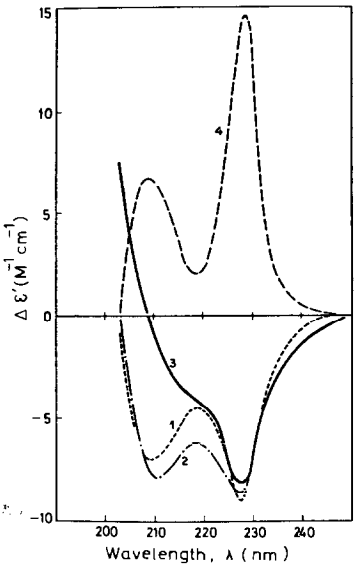

FIG. 1. CD spectra (200–250 nm in dioxane) (7) of individual gramicidin species.

The CD spectra of gramicidin A and its analogs in dioxane are represented in Figs. 1–5. The dependence of $\Delta\epsilon'_{228} - \log c$ and the theoretical curves for the monomer–dimer transition are also given for those cases where the concentrational changes in the CD spectra are sufficient for determining the dimerization constant. In Table 1, dimerization constants for the gramicidin A analogs determined by two independent methods are listed. At the same time it was observed that for analogs (5) and (4) at $c \geqslant 10^{-2} M$ in ethanol, the $\Delta\epsilon'_{228} - \log c$ and $d - \log c$ curves deviate from S shape. This is illustrated in Fig. 5 where the CD spectra and the deviation of $\Delta\epsilon'_{228}$ vs log c from the theoretical S-shaped curve is shown for analog (5) in ethanol. It would be natural to assume that such deviations are caused by the competitive formation of trimeric or higher aggregates after reaching a certain concentration. In these cases K_{dim} was determined only from the initial portion of the $\Delta\epsilon' - \log c$ curve (points 1–6, Fig. 6), and the theoretical

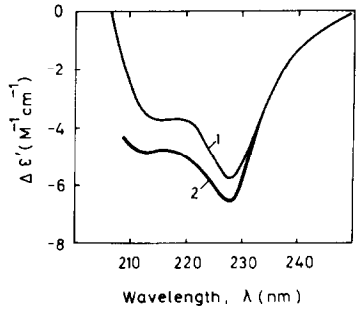

FIG. 2. CD spectra (200–250 nm) of gramicidin A under equilibrium conditions in dioxane. (1) $c = 7.75 \times 10^{-4} M$. (2) $c = 1.0 \times 10^{-3} M$.

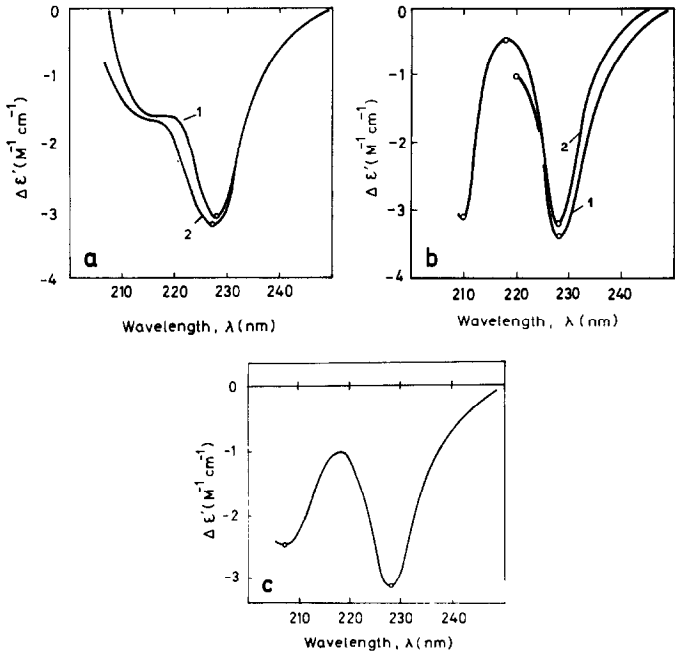

FIG. 3. CD spectra (200–250 nm) of gramicidin analogs (2), (4), (5) with the number of residues $N \geq 13$ in dioxane. (a) Analog (5): curve 1, $c = 1,0 \times 10^{-2} M$; curve 2 $c = 1,0 \times 10^{-4} M$. (b) Analog (2): curve 1 $c = 1,0 \times 10^{-4} M$; curve 2, $c = 1,0 \times 10^{-3}$–$1,0 \times 10^{-2} M$. (c) Analog (4): $c = 9,0 \times 10^{-5}$–$1,0 \times 10^{-3} M$.

curve for the comparison was plotted accordingly. A sharp decrease in band intensity in the CD spectra due to aggregation of order $N > 2$ could be observed in some cases in dioxane (Fig. 6a); however, such aggregation begins only after dimerization of the analogs.

Let us consider the CD spectra of gramicidin A analogs that at $10^{-3} M$ dioxane are almost 100% dimerized. One may clearly observe similarity of the dimer curves of analogs (3, 5–7) (Figs. 3a and 4) with the dimeric spectra of gramicidin A (Fig. 1). Quantitation in terms of the four dimer species of gramicidin A analogs presented certain difficulties because of the variations in both the overall number of residues and the number of tryptophans. However, it was found on comparing the CD spectra of gramicidin A (Fig. 2) and hydrogenated gramicidin A (*22*) (where Trp is replaced with the respective perhydroindole derivative) that the peptide contribution to the Cotton effect at 228 nm amounted to less than 0.3 of the overall effect, which could thus be ascribed mainly to the tryptophan residues (8 Trp out of 30 residues in the dimer). The peptide contribution to the effect in the 210 to 220-nm region could be found from the spectrum of species 3 (Fig. 1), differing from that of the other forms in the absence of the 210-nm band (evidently because there are no tryptophan contributions in that region). Assuming that the 228-nm band is symmetric, one could thus easily isolate the peptide part of the spectrum as shown in Fig. 7. The part that is isolated is close to the spectrum of hydrogenated derivative of the antibiotic (*22*). The strong Trp component of the

TABLE 1

STABILITIES AND STRUCTURES OF THE DIMERS OF GRAMICIDIN A AND OF ITS ANALOGS

Prevailing species	No.	Compound[a,b]	Number of residues	Relative concentration of gramicidin A individual species at equilibrium in dioxan (%)			Dimerization constant			
							Dioxane		Ethanol	
							CD	FP	CD	FP
		Form VGALAVVVTLTLTLT $NHCH_2CH_2OH$	15	1 + 2	3	4	—	$\sim 10^5$	—	3×10^4
		Gramicidin A[c]		46	42	13				
3	5	Form VGALAVVV–TLTLT $NHCH_2CH_2OH$	13	21 ± 6	*54* ± 7	25 ± 12	—	$(4.0 \pm 0.5) \times 10^3$	$(3.0 \pm 0.4) \times 10^2$	$(3.5 \pm 1.0) \times 10^2$
	6	Form VGALAVVV–TLTNHCH_2CH_2OH	11	8 ± 2	*92* ± 3	2 ± 2	$(9.6 \pm 0.5) \times 10^4$	$\sim 10^5$	$(1.4 \pm 0.4) \times 10^2$	$(2.0 \pm 1.0) \times 10^2$
4	3	Form VGVLVLVLTLTLTLTNHCH_2CH_2OH	15	0	20 ± 5	*80* ± 5	$\sim 10^5$	$(4.0 \pm 1.5) \times 10^4$	$(3.0 \pm 2.0) \times 10^4$	$(9.0 \pm 3.0) \times 10^3$
	7	Form VG–VVTLTLTLTNHCH_2CH_2OH	11	4 ± 4	0	*96* ± 4	$(1.6 \pm 0.4) \times 10^5$	$\sim 10^5$	$(3.0 \pm 1.0) \times 10^2$	$\sim 10^3$
	8	Form VG–TLTLTLTNCH_2CH_2OH	9	35 ± 2	0	65 ± 2	$(3.5 \pm 2.0) \times 10^3$	$(2.6 \pm 2.0) \times 10^3$	$(1.0 \pm 0.5) \times 10^2$	$\sim 10^2$
1 + 2	4	Form VGALAV–TLTLTLTNCH_2CH_2OH	13	48 ± 16	22 ± 18	30 ± 30	—	$(5.5 \pm 0.5) \times 10^2$	$(2.5 \pm 0.5) \times 10^2$	$(3.0 \pm 1.0) \times 10^2$
	2	Form LVGALAVVVTLTLTLTNCH_2CH_2OH	16	52 ± 16	28 ± 17	20 ± 20	—	$\sim 10^3$	$(3.2 \pm 0.7) \times 10^2$	$(3.8 \pm 0.5) \times 10^2$
—	1	Form VGALAVVVGTLTLTLTNHCH_2CH_2OH	16	No species of gramicidin A			—	—	—	$< 10^3$

[a] Amino acids are designated by single letter symbols: V, Val; G, Gly; A, Ala; L, Leu; T, Trp.

[b] Modified sites are italicized and deleted ones replaced by lines.

[c] Data from Ref. (*8*).

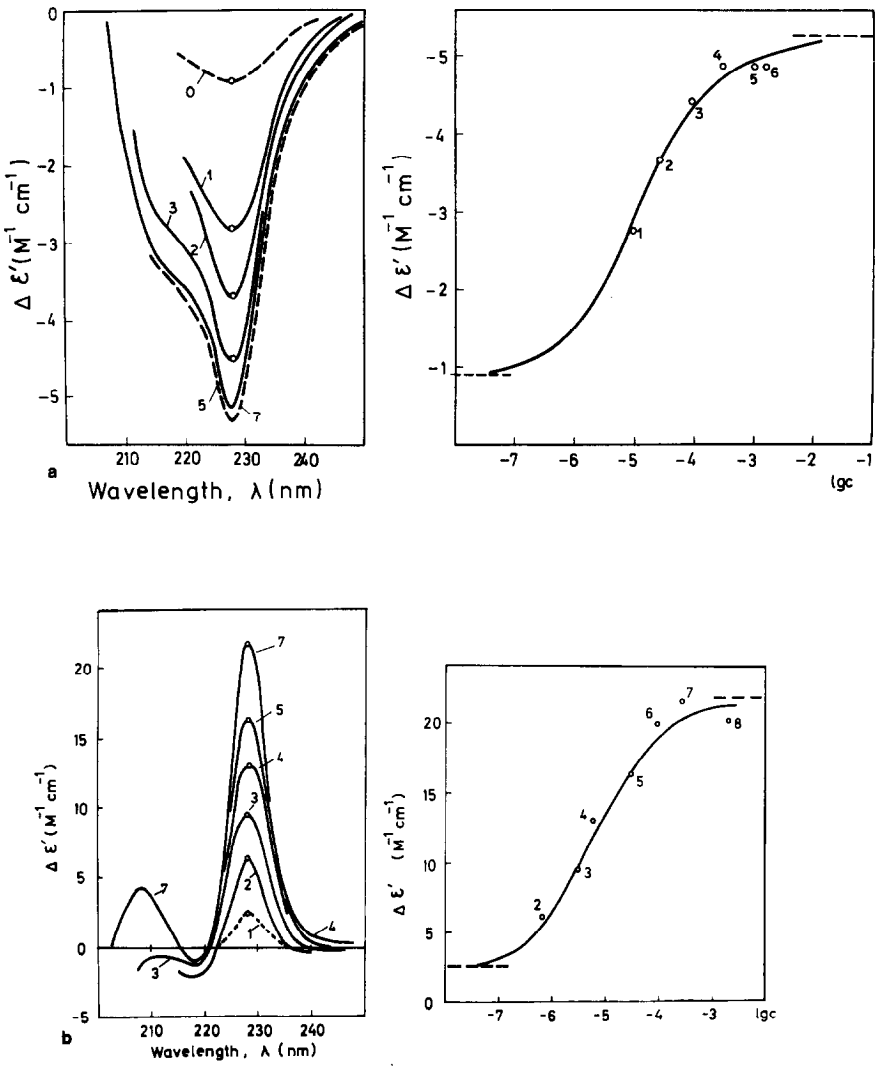

FIG. 4. On the left, CD spectra of gramicidin analogs (3), (6)–(8) in dioxane. On the right, corresponding concentration dependences of $\Delta\epsilon'_{228}$. The line is the theoretical dimerization curve. (a) Analog (6): (0) corrected for 100% monomer, (7) corrected for 100% dimer. (b) Analog (7); (1) corrected for 100% monomer. (c) Analog (3): (1) corrected for 100% monomer. (d) Analog (8): (7) corrected for 100% dimer.

CD spectra of the analogs varying in accordance with the number of Trp residues was then renormalized with respect to these residues, leaving the weak peptide component uncorrected. The two components were then added to give the overall spectrum. Such corrections were made for the spectra of all the four gramicidin A species and of its analogs (in the case of species 4 and of analogs with positive Cotton effects, the mirror image of the weak component of species 3 was taken).

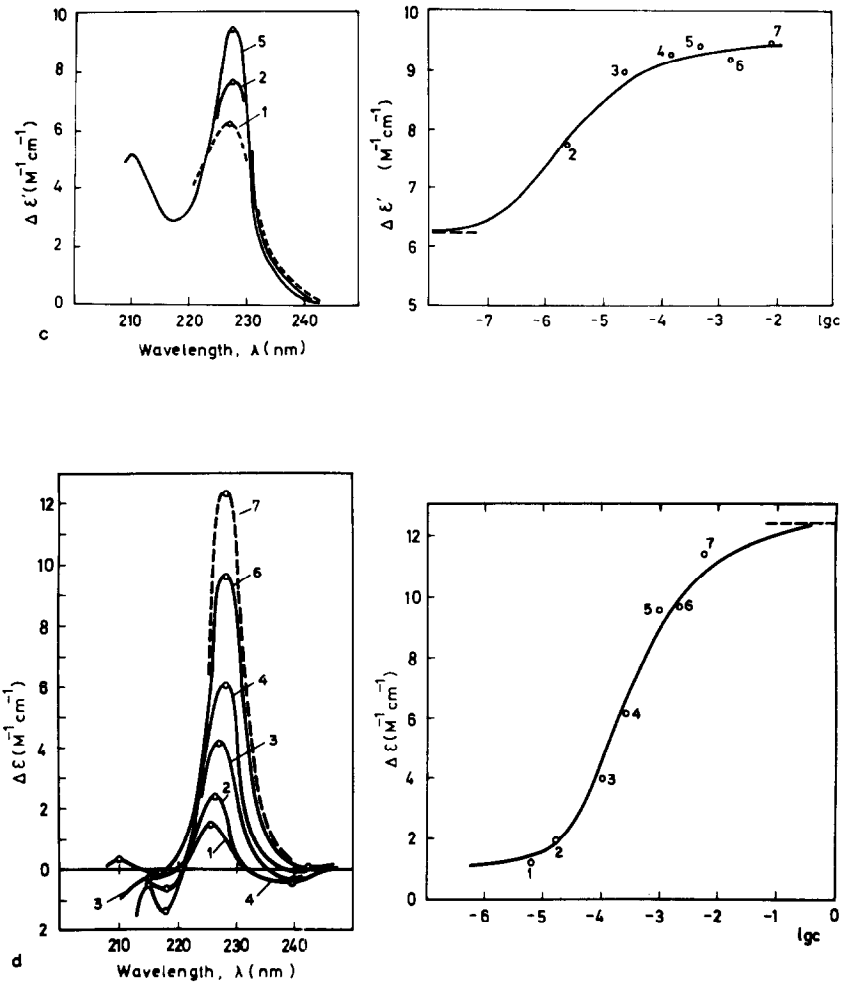

FIG. 4.—*continued*

Optimal fit of the CD spectrum of the analog was then found algebraically by linear combination of the spectra of the gramicidin A species. The results are presented in Table 1 where the analogs are listed in groups within each of which the dimer species indicated in the table is predominant. The species contents of the analogs determined by CD are in qualitative agreement with the results of thin layer chromatography obtained by Veatch (*23*) with analogs (4)–(8). Thus, analog (6) displayed a single spot with R_f corresponding to that of species 3, whereas analog (4) showed the presence of species 1–4 with species 2 predominant, etc. The rapid interconversion of the species in the analogs precludes their quantitative determination by thin layer chromatography (*23*).

The CD spectra of the third group analogs (Table 1) cannot be sufficiently accurately described by a linear combination of the spectra for species and relative concentration of species 3 and 4 were large root mean square deviations.

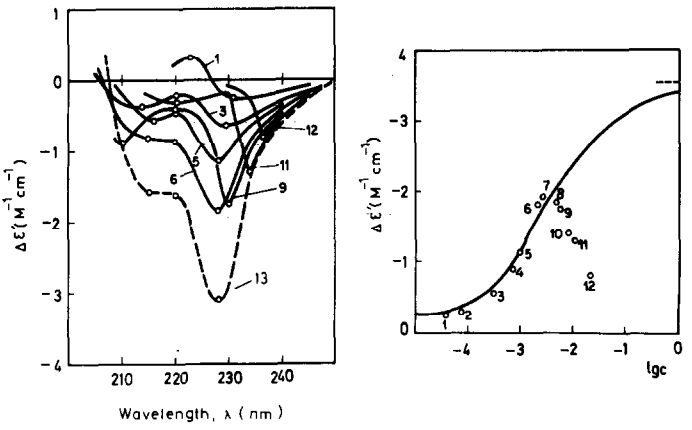

FIG. 5. On the left, CD of analog (5) in ethanol. Point 13, corrected for 100% dimer. On the right, concentrational dependence of $\Delta\epsilon'$. Point 9 and the following ones are $\Delta\epsilon'$ values at the minimum of the curve and not at 228 nm. The line is the theoretical dimerization curve.

For these analogs it could only be said that the contribution from species 1 and 2 is predominant (Table 1).

The CD spectrum (not shown) of compound (1) has a peak intensity of only ca. 0.1 that of the peaks of the gramicidin A species. This spectrum cannot be described by a linear combination of the spectra of the species, evidence that they are absent from the solution of this analog.

A study of the conformational equilibrium in the gramicidin A analogs made it possible to follow the relationship between the relative amounts of the species on

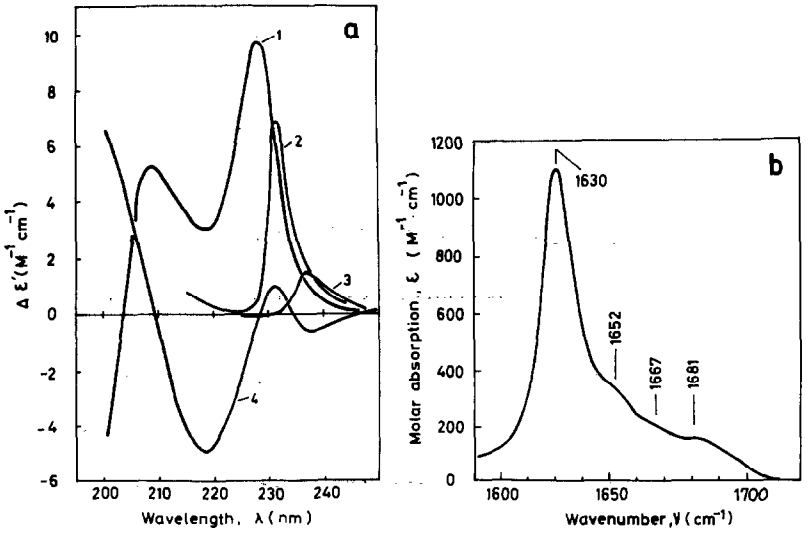

FIG. 6. (a) CD spectra of analogs (3) (curves 1, 2, 3) and (6) (curve 4) in dioxane for higher-than-dimer concentrations (1) $c = 6.9 \times 10^{-3} M$. (2) $c = 2.6 \times 10^{-2} M$. (3) $c = 7.8 \times 10^{-2} M$. (4) $c = 1.2 \times 10^{-3} M$. (b) Infrared spectrum of analog (6) in dioxane for $c = 1.2 \times 10^{-3} M$.

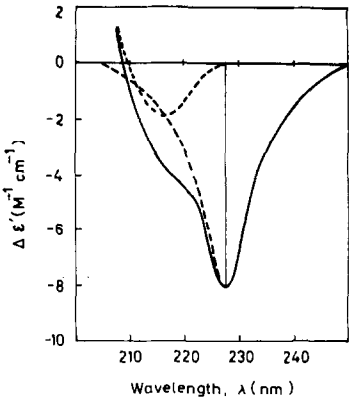

FIG. 7. Isolation of the symmetric component at 228 nm in the CD spectrum of gramicidin species 3 in dioxane.

the one hand and the primary structures of the analogs on the other. It turned out that if on shortening the molecule the "tail" end of the gramicidin A sequence $(TL)_3T$ is retained the conformational equilibrium is shifted in the direction of species 4 in analogs (7 and 8) and of species 1 + 2 in analog (4). On the contrary, a decrease in Trp content in analogs (5) and (6) shifts the equilibrium in the direction of species 3. Interestingly, compounds (6) and (7) consist practically entirely of species 3 and 4, respectively. From this it follows that analogs can be synthesized to give individual species.

Infrared Spectra (Experiment)

Infrared spectra of the analogs and gramicidin A species 3 in dioxane were obtained at "dimeric" concentrations (Figs. 8–10). Since for the present study we had to know not only the shape of the spectrum, but also the intensities of the amide I bands we could not use the spectra of the species in chloroform, obtained earlier (*7*).

The ir spectra in the amide I and amide II regions are of the same type for all analogs and also for species 3 (Figs. 8–10). They all display an intense amide I maximum at 1634–1638 cm^{-1} with a molar absorption coefficient of ϵ = 600–800 M^{-1}, a shoulder at about 1646–1650 cm^{-1}, and a high frequency component at 1690 cm^{-1}.

In addition, in the ir spectra of analogs (5) and (6) (species 3), and (7) (species 4) one or two high frequency components can be observed with maxima at about 1665–1670 cm^{-1} and 1680 cm^{-1} (Figs. 8–10). However, there is no apparent relationship between the relative intensity of these bands and the predominance of species 3 or 4.

The ir spectra of analogs (4) and (2) differ from those of species 3 and of the analogs of corresponding lengths of the first two groups (Table 1) in having higher frequencies of the main component (by 2–3 cm^{-1}). Also in dioxane they display a weak but distinct band at about 1720 cm^{-1} which in chloroform is shifted to 1709

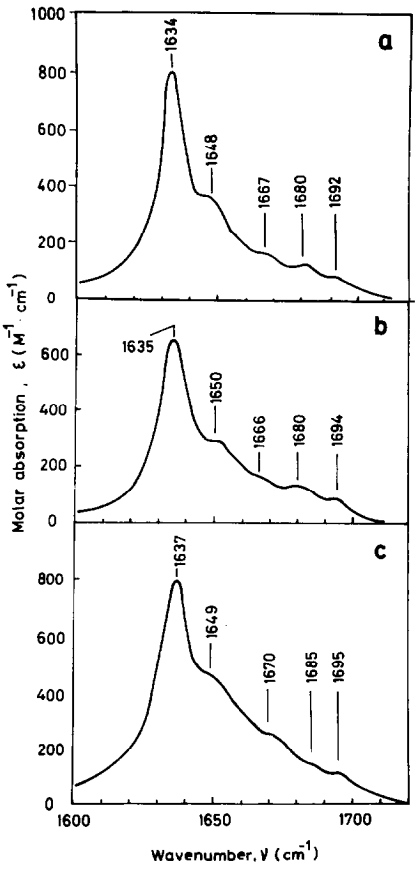

FIG. 8. Infrared spectra in dioxane of gramicidin species 3 and of analogs, containing predominantly this species. The relative dimer content for the given concentration is shown in parentheses. (a) Gramicidin (species 3), $c = 1.95 \times 10^{-3} M$ (95%). (b) Analog (5), $c = 2.0 \times 10^{-2} M$ (93%). (c) Analog (6), $c = 9.55 \times 10^{-4} M$ (93%).

cm^{-1}. The 1720-cm^{-1} band absent from the spectra of all other analogs and of species 3, is due to absorption by the non-hydrogen-bonded formamide carbonyl (*24*). The amide I band of analog (1) (not shown here) has a frequency of about 1640 cm^{-1}, is relatively weak ($\epsilon = 280 M^{-1} cm^{-1}$) and broad ($\Delta\nu_{\frac{1}{2}} = 50 cm^{-1}$). In the region of the amide II frequencies a 1534-cm^{-1} component instead of the usual ~1545 cm^{-1} component appears, i.e., the amide I and amide II regions of the spectrum of analog (1) differ greatly from those of all other analogs.

We now consider the ir spectra of the monomers. The high dimerization constant (10^5 in dioxane) of gramicidin A itself and of analogs (3), (6), and (7) precludes the recording of the spectra for predominantly monomeric species of these compounds in nonpolar media. For this we, therefore, made use of analogs (5) and (8) whose K_{dim} values are considerably lower (Table 1). A monomer ir spectrum could be obtained in dioxane solution for analog (5) that at a concentration of $10^{-4} M$ had a monomer:dimer ratio of 65:35 (Fig. 11). The monomer

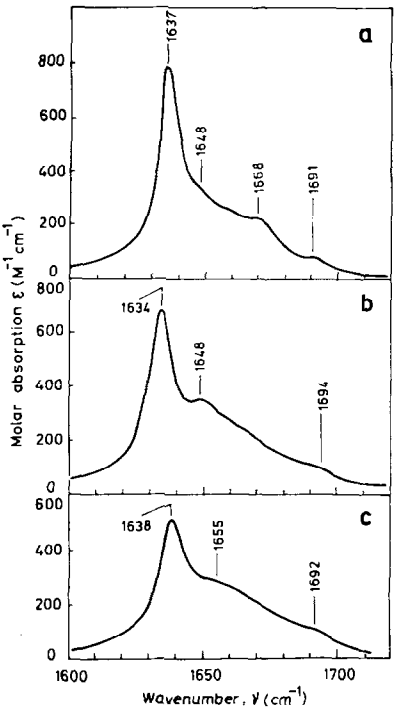

FIG. 9. Infrared spectra in dioxane of gramicidin analogs containing predominantly species 4. The relative dimer content for the given concentration is shown in parentheses. (a) Analog (7), = 1.0×10^{-2} *M* (98%). (b) Analog (3), $c = 7.65 \times 10^{-3}$ *M* (98%). (c) Analog (8), $c = 2.05 \times 10^{-2}$ *M* (92%).

spectrum was obtained from this spectrum by subtracting the absorption of the 35% dimer (whose spectrum was known). In the resultant spectrum the principal component frequency is about 1653 cm^{-1}. The spectrum of analog (8) has the same component at the same dilution but in general the amide I band is considerably broadened ($\Delta\nu_{\frac{1}{2}} = 50$ cm^{-1}), and moreover the amide II maximum is shifted to 1637 cm^{-1}, evidence of an unordered structure of this shortened analog (*25*).

The ir spectra in dioxane for gramicidin A and analogs (3), (6), and (7) were

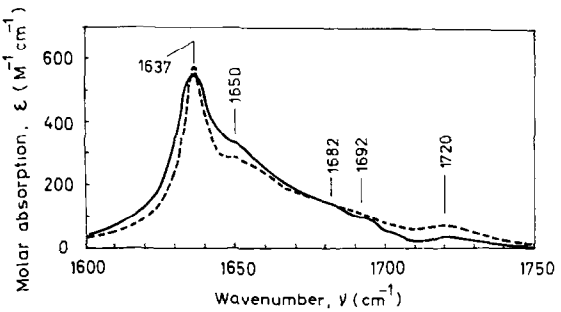

FIG. 10. Infrared spectra in dioxane of gramicidin analogs with predominant species 1. + 2. The relative dimer content for the given concentration is shown in parentheses. Dotted line, analog (2), $c = 2.0 \times 10^{-2}$ *M* (86%). Continuous line, analog (4), $c = 2.0 \times 10^{-2}$ *M* (81%).

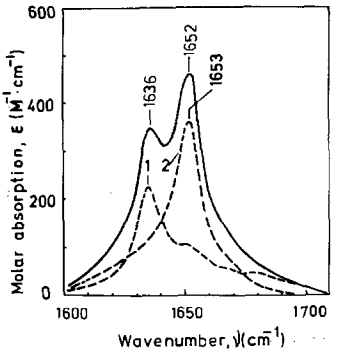

FIG. 11. Resolution of the observed ir spectrum of analog (5) in dioxane at $c = 1.0 \times 10^{-4} M$ (65% monomer) into monomeric and dimeric components. (1) Dimer absorption; (2) monomer absorption.

obtained at $10^{-5} M$ concentrations, i.e., for a 50 : 50 monomer : dimer ratio. Figure 12 shows the spectrum of gramicidin A wherein there can be seen a component at 1650 cm^{-1}.

The accuracy of measuring the ir spectra at 10^{-5} M concentrations is insufficient, however, for quantitative analysis of the bands. At the same time the considerable difference in main peak positions for the monomer and the dimer made possible observation of the kinetics of transition from 100% dimer to the state of 50% dimer : 50% monomer using the intensity ratios of the 1650- to 1653- and 1634- to 1636-cm^{-1} bands. The half-times of these transitions are presented in Table 2.

Infrared Spectra (Calculation)

The amide I frequencies in the ir spectra were calculated for the following gramicidin A conformations:

(1) antiparallel double helices with 5.6, 7.2, and 9.0 residues per turn, i.e., $\uparrow\downarrow\pi\pi^{5.6}_{LD}$, $\uparrow\downarrow\pi\pi^{7.2}_{LD}$, and $\uparrow\downarrow\pi\pi^{9.0}_{LD}$;

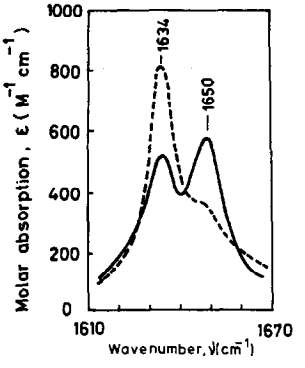

FIG. 12. Continuous line, ir spectrum of gramicidin A in dioxane for $c = 1.0 \times 10^{-5} M$ (~50% dimer + ~50% monomer). Dotted line, ir spectrum of species 3 (for comparison).

TABLE 2

HALF-TIMES FOR THE DIMER → 0.5 DIMER + 0.5 MONOMER TRANSITION OF GRAMICIDIN A AND ITS ANALOGS IN DIOXANE

Compound	*N*	Half-times
Gramicidin A species 3	15	~ 4 days
Analog		
3	15	>15 days
5	13	~10 min
7	11	~20 min
6	11	~ 3 min

(2) parallel double helices with 5.6 and 7.2 residues per turn, i.e., $\uparrow\uparrow\pi\pi_{LD}^{5.6}$ and $\uparrow\uparrow\pi\pi_{LD}^{7.2}$.

(3) π_{LD} helices with 4.4 and 6.3 residues per turn joined in a head-to-head fashion, i.e., $\overrightarrow{\pi_{LD}^{4.4}}\,\overleftarrow{\pi_{LD}^{4.4}}$ and $\overrightarrow{\pi_{LD}^{6.3}}$ and $\overleftarrow{\pi_{LD}^{6.3}}$.

(4) π_{LD} helices with 4.4 and 6.3 residues per turn joined in a head-to-tail fashion, i.e., $\overrightarrow{\pi_{LD}^{4.4}}\,\overrightarrow{\pi_{LD}^{4.4}}$ and $\overrightarrow{\pi_{LD}^{6.3}}\,\overrightarrow{\pi_{LD}^{6.3}}$.

(5) Monomer in the $\pi_{LD}^{4.4}$ and $\pi_{LD}^{6.3}$ conformations.

The atomic coordinates for the antiparallel double helices and the $\pi_{LD}^{4.4}$ structure were taken from Ref. (*13*). The atomic coordinates for the $\pi_{LD}^{6.3}$, $\uparrow\uparrow\pi\pi_{LD}^{5.6}$, and $\uparrow\uparrow\pi\pi_{LD}^{7.2}$ helices were kindly communicated by Dr. F. Colonna-Cesari. For the $\overrightarrow{\pi_{LD}}\,\overrightarrow{\pi_{LD}}$ dimers the atomic coordinates were obtained by simply doubling the length of the respective π_{LD} monomeric helix. For plotting the coordinates of the second helix in the $\overrightarrow{\pi_{LD}}\,\overleftarrow{\pi_{LD}}$ type dimer use was made of the existence of a twofold axis perpendicular to the helical axes at the site of junction of the units. In order to determine the position of this axis the $\Delta\phi$ and ΔZ values were obtained with Dreiding models, permitting transition from the cylindrical coordinates of the formamide carbon atom of the first unit to the corresponding coordinates of the second unit.

Resonance interaction of the amide I vibrations for the helical models of gramicidin A were treated by perturbation theory (*26*) in the dipole–dipole approximation. The method of calculation and the parameters of the transition dipole moment as also the magnitude, direction, and location of its center were taken from Chirgadze and Nevskaya (*19–21*); for the $\uparrow\downarrow\pi\pi_{LD}$ and $\uparrow\uparrow\pi\pi_{LD}$ helices they were considered to be the same as for the β-structures (*19, 20*), and for the π_{LD} helices, the same as for an α-helix (*21*). To determine the frequencies of the individual amide bands we used the formula

$$\nu = \nu_0 + \Delta\nu_{res},$$

where ν_0 is the vibration frequency of the unperturbed resonance interaction, and $\Delta\nu_{res}$ is the resonance shift of the frequency relative to ν_0.

The calculated ir spectra (Figs. 13–17) were obtained in the relative scale with

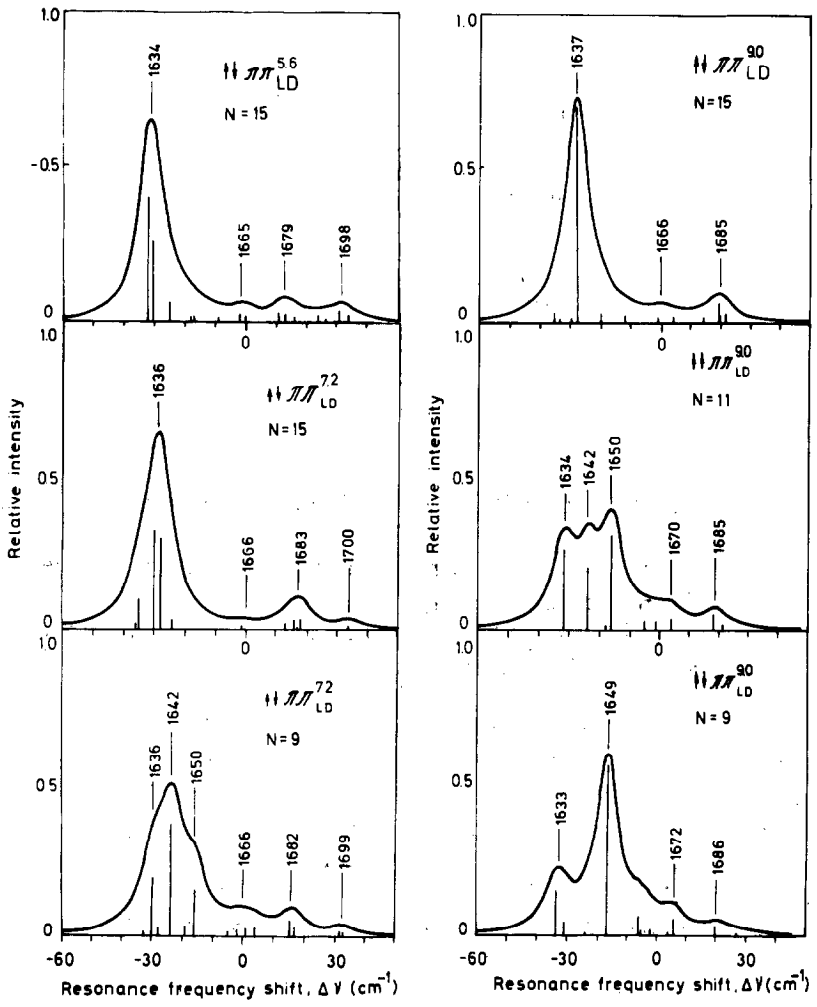

FIG. 13. Calculated ir spectra of the amide I vibration in the $\uparrow\downarrow\pi\pi_{LD}$ helices.

the unperturbed frequency ν_0 taken as 0. In order to pass over to the practical scale the appropriate value for ν_0 had to be selected. For the antiparallel double helices this was done by comparison of the calculated and observed bandshapes. As noted earlier, in the spectrum of gramicidin A (Fig. 8a) and of certain of the 9, 11-, and 13-membered analogs (Figs. 8–10) a strong low frequency component (1634–1638 cm^{-1} and a series of weaker components at higher wave numbers can be observed. Of all the calculated spectra, only those for the $\uparrow\downarrow\pi\pi^{5,6}_{LD}$ helices with $N = 9$, 11, 13, and 15 (Fig. 13) have all these components. On one hand, this fact serves as a structural probe (see below), and on the other, gives rise to a $\nu_0(\uparrow\downarrow\pi\pi_{LD})$ value of 1666 cm^{-1}.

The same value should be taken for the parallel double helices (*19, 20*). In obtaining ν_0 for the single strand π_{LD} helices, we utilized the amide frequency obtained for poly(γ-benzyl-DL-glutamate) in the $\pi^{4.8}_{L}$ conformation of the helix (*13*). For the polymer of molecular weight 30,000 (i.e., about 120 residues) the

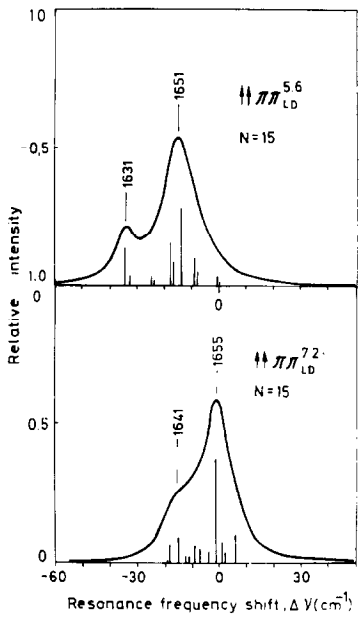

FIG. 14. Calculated ir spectra of the amide I vibration in the $\uparrow\uparrow \pi\pi_{LD}$ helices.

frequency found was 1645 cm^{-1}. We calculated the ir spectra of $\pi_{LD}^{4,4}$ helices of various lengths. The result of the calculation is shown in Fig. 18, wherein it can be seen that for a polymer (for instance with $N = 120$) $\Delta\nu_{res} = -25$ cm^{-1}. This gives $\nu_0(\pi_{LD}) = 1670$ cm^{-1}.

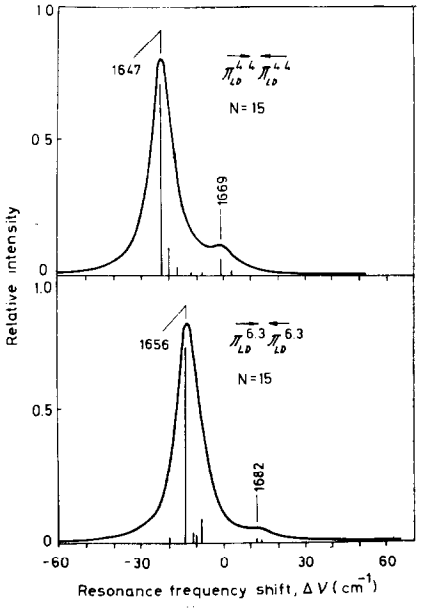

FIG. 15. Calculated ir spectra of the amide I vibration in the $\overrightarrow{\pi_{LD}^{4,4}}\,\overleftarrow{\pi_{LD}^{4,4}}$ and $\overrightarrow{\pi_{LD}^{6,3}}\,\overleftarrow{\pi_{LD}^{6,3}}$ dimers.

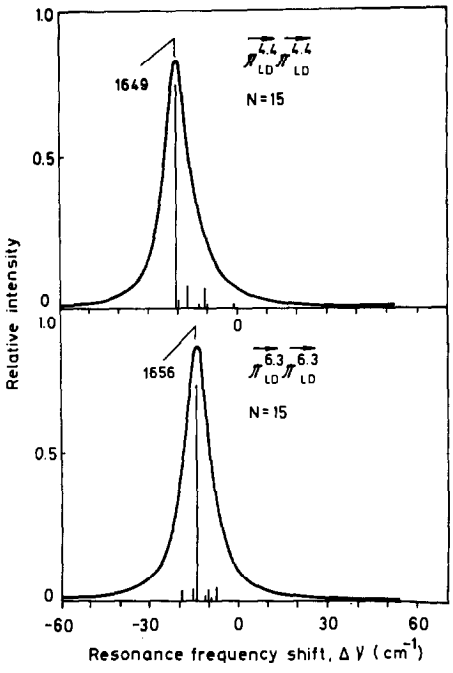

FIG. 16. Calculated ir spectra of the amide I vibration in the $\overrightarrow{\pi^{4.4}_{LD}}\,\overrightarrow{\pi^{4.4}_{LD}}$ and $\overrightarrow{\pi^{6.3}_{LD}}\,\overrightarrow{\pi^{6.3}_{LD}}$ dimers.

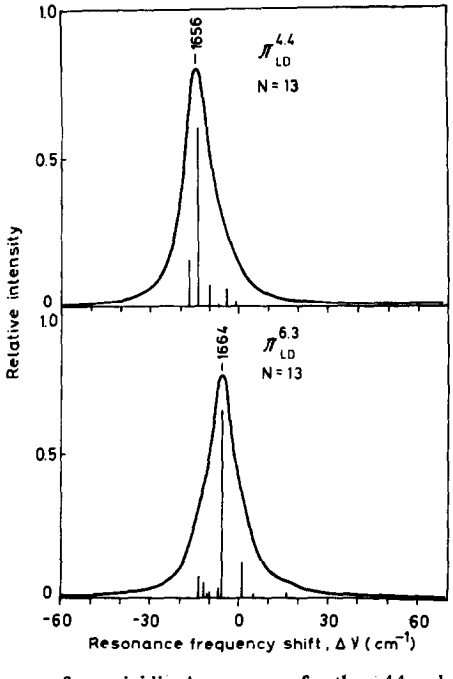

FIG. 17. Calculated ir spectra of gramicidin A monomer for the $\pi^{4.4}_{LD}$ and $\pi^{6.3}_{LD}$ helical conformations.

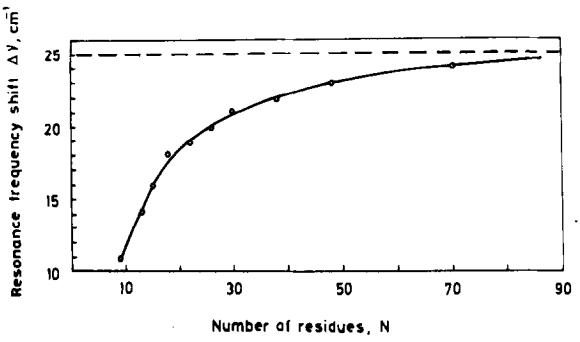

FIG. 18. Dependence on the chain length of the resonance shift of the main component frequency in the calculated ir spectrum of the $\pi^{4,4}_{LD}$ helix.

The main component frequencies of all the helical structures are presented in Table 3. Since gramicidin A analogs of various lengths were studied (Table 1) calculation of the ir spectra of all the structures was carried out for chains of 15 to 9 residues (and with account of the terminal groups). With most structures significant changes in the shape of the amide I band do not occur on chain shortening, only small frequency shifts of the individual components being observed. The calculated spectra of the chain-shortened analogs are presented only in those cases when such shortening changes the bandshape.

Comparison of the calculated ir spectra shows that the lowest main component frequencies are possessed by the antiparallel double helices, the frequency shifting to lower wavelengths as the helical diameter increases from 1634–1638 cm^{-1} for $\uparrow\downarrow\pi\pi^{5,6}_{LD}$ to 1637–1649 cm^{-1} for $\uparrow\downarrow\pi\pi^{9,0}_{LD}$. In the case of the $\uparrow\downarrow\pi\pi^{7,2}_{LD}$ helix two shoulders appear in the profile of the strong component at 1640 cm^{-1} at $N = 9$. The spectra of $\uparrow\downarrow\pi\pi^{9,0}_{LD}$ helices are even more sensitive to chain length (Fig. 13); also noteworthy is the absence of a 1700-cm^{-1} component.

TABLE 3

CALCULATED FREQUENCIES OF THE MAIN AMIDE I BAND COMPONENTS (cm^{-1})

Conformation	Number of residues (N)			
	15	13	11	9
$\uparrow\downarrow\pi\pi^{5,6}_{LD}$	1634	1635	1636	1638
$\uparrow\downarrow\pi\pi^{7,2}_{LD}$	1636	1638	1639	1640
$\uparrow\downarrow\pi\pi^{9,0}_{LD}$	1637	1638	1634, 1642, 1650	1649
$\uparrow\uparrow\pi\pi^{5,6}_{LD}$	1651	1652	1652	1656
$\uparrow\uparrow\pi\pi^{7,2}_{LD}$	1655	1659	1660	1661
$\overrightarrow{\pi^{4,4}_{LD}}\ \overleftarrow{\pi^{4,4}_{LD}}$	1647	1647	1648	1650
$\overrightarrow{\pi^{6,3}_{LD}}\ \overleftarrow{\pi^{6,3}_{LD}}$	1656	1657	1659	1661
$\overrightarrow{\pi^{4,4}_{LD}}\ \overleftarrow{\pi^{4,3}_{LD}}$	1649	1650	1651	1652
$\overrightarrow{\pi^{6,3}_{LD}}\ \overleftarrow{\pi^{6,3}_{LD}}$	1656	1657	1658	1660
$\pi^{4,4}_{LD}$	1654	1656	—	1659
$\pi^{6,3}_{LD}$	1663	1664	—	1670

The spectrum of the $\uparrow\uparrow\pi\pi^{5,6}_{LD}$ helix (Fig. 14) has a strong component at about 1652–1657 cm^{-1} and a weak low-frequency component at 1632–1635 cm^{-1}. The spectrum of the $\uparrow\uparrow\pi\pi^{7,2}_{LD}$ helix is sensitive to N and has higher frequencies for both the strong and the weak components (Fig. 14).

The frequencies of the strong components in the spectra calculated for both the symmetric $\overrightarrow{\pi_{LD}}\,\overleftarrow{\pi_{LD}}$ and the unsymmetric $\overrightarrow{\pi_{LD}}\,\overrightarrow{\pi_{LD}}$ dimers practically coincide. In addition in the spectra of the $\overrightarrow{\pi^{4,4}_{LD}}\,\overleftarrow{\pi^{4,4}_{LD}}$ and $\overrightarrow{\pi^{6,3}_{LD}}\,\overleftarrow{\pi^{6,3}_{LD}}$ structures there is a weak high-frequency component at ca. 1669 and 1682 cm^{-1}, respectively.

Finally the ir spectra evaluated for the monomers in the $\pi^{4,4}_{LD}$ and $\pi^{6,3}_{LD}$ conformations are shown in Fig. 17. In both cases one observes an almost symmetric band shape, however its frequency for the $\pi^{6,3}_{LD}$ helix is significantly higher than for the $\pi^{4,4}_{LD}$ helix.

DISCUSSION

Conformational Equilibrium of Gramicidin A in Solution

The amide I ir regions of gramicidin A and of its analogs are all similar. On the other hand calculations predict a high susceptibility of the ir spectra to changes in the helical conformation. From this it follows that all the species must have a similar structural type for the polypeptide backbone. The differences between the individual species could thus be associated with changes in the sign of rotation of the helix or differences of side change orientations. The answer to the question of what actually is the structure is given by comparison of the calculated and observed amide I ir frequencies.

As already noted the observed ir spectra for all the analogs and conformational species of gramicidin A have a main component with a maximum at 1634–1638 cm^{-1}. The amide I band in the spectrum calculated for both the symmetric $\overrightarrow{\pi_{LD}}\,\overleftarrow{\pi_{LD}}$ and the unsymmetric $\overrightarrow{\pi_{LD}}\,\overrightarrow{\pi_{LD}}$ dimers has a frequency in the range 1647–1661 cm^{-1} (Table 3), which is thus far from the experimental values. Consequently these conformations are not the preferable ones for the gramicidin A dimer. The same can be said of the $\uparrow\uparrow\pi\pi_{LD}$ helices, the calculated spectra (Fig. 14) of which differ considerably from the experimental in the intensity ratios of the low to high frequencies. We do not present the spectra for the $\uparrow\uparrow\pi\pi_{LD}$ helices of diameter larger than that of a $\uparrow\uparrow\pi\pi^{7,2}_{LD}$ helix, because conformational calculations showed them to be unstable (*27*).

The spectra of the $\uparrow\downarrow\pi\pi_{LD}$ helices are in better agreement with the experimental spectra of the analogs and of species 3 than those of all other models. However, in the theoretical spectra of these dimer models the shoulder at 1648 cm^{-1} is absent (Fig. 13), whereas it is observed in all the gramicidin A and its analog (13) (N = 15), corresponding to increased frequency of this component in the theoretical spectra of the $\uparrow\downarrow\pi\pi^{7,2}_{LD}$ helix compared to the $\uparrow\downarrow\pi\pi^{5,6}_{LD}$ helix (Table 3). In the analogs modeling species 3 or 4 the 1720-cm^{-1} band is absent, evidence of the absence of a $\uparrow\downarrow\pi\pi^{7,2}_{LD}$ helix. In the case of species 4 this is substantiated in the experimental spectrum of the chain-shortened analog (7) (N = 9) by the absence of a low-

frequency shoulder at ca. 1636 cm^{-1} characteristic of that calculated for a $\uparrow\downarrow\pi\pi^{7.2}_{LD}$ helix with $N = 9$ (Fig. 13).

We thus have all grounds to assume that the basic conformation of species 1 + 2 is the $\uparrow\downarrow\pi\pi^{7.2}_{LD}$ helix, while for species 3 and 4 it is the $\uparrow\downarrow\pi\pi^{5.6}_{LD}$ helix. This conclusion is in keeping with the latest X-ray data (*28*), according to which the gramicidin A helix in the crystal (species 3 (*7*) has a length of ca. 32 Å and a diameter of ~5 Å, conforming closest to a $\uparrow\downarrow\pi\pi^{5.6}_{LD}$ helix (*7*).

The spectrum of analog (4) differs from that of analog (2) by an approximately twofold decrease in intensity of the 1720-cm^{-1} band and a broadening of the main component (1636.5 cm^{-1}). Such intensity change could be due to ca. half the molecules of the peptide being in the $\uparrow\downarrow\pi\pi^{7.2}_{LD}$ helical conformation and the other half in the $\uparrow\downarrow\pi\pi^{5.6}_{LD}$ conformation. According to the calculations the presence of both helices should lead to broadening of the main component of the amide I band because of the 2–3 cm^{-1} difference in the $\uparrow\downarrow\pi\pi^{5.6}_{LD}$ and $\uparrow\downarrow\pi\pi^{7.2}_{LD}$ frequencies, as can be observed in the spectrum of analog (4) (Fig. 10).

The calculated spectra of models $\uparrow\downarrow\pi\pi^{5.6}_{LD}$ and $\uparrow\downarrow\pi\pi^{7.2}_{LD}$ do not contain the shoulder of 1648 cm^{-1} observed in the spectra of all analogs and species of gramicidin A (its cause will be discussed presently). In the calculated spectra of the $\uparrow\downarrow\pi\pi^{9.0}_{LD}$ helix, contrary to the observed spectra, there is no third high-frequency component (Fig. 13); and, what is more important, the spectra are susceptible to chain shortening so that for, say, $N = 11$ the calculated spectra are completely different from those experimentally observed for analogs (7) and (6) of corresponding length. Hence, by varying the chain length of gramicidin A and making the respective calculation in the series of the resultant analogs, the conclusion follows that there is no $\uparrow\downarrow\pi\pi^{9.0}_{LD}$ conformation in the gramicidin A solution. The spectra of the $\uparrow\downarrow\pi\pi^{5.6}_{LD}$ and $\uparrow\downarrow\pi\pi^{7.2}_{LD}$ helices are in agreement with the observed ir spectra of gramicidin A and its analogs for different chain lengths, meaning that the predominant conformations of gramicidin A in nonpolar solvents could be $\uparrow\downarrow\pi\pi^{5.6}_{LD}$ and $\uparrow\downarrow\pi\pi^{7.2}_{LD}$ helices.

In the ir spectra of the species (1 + 2)-enriched analogs (2) and (4) a band (1720 cm^{-1} in dioxane) corresponding to the free formamide carbonyl vibration is displayed. The absence of this band in the spectra of other analogs and of species 3 is due to H bonding of the carbonyl by the terminal ethanolamide OH group of the second chain, which is possible in a $\uparrow\downarrow\pi\pi^{5.6}_{LD}$ helix. In the $\uparrow\downarrow\pi\pi^{7.2}_{LD}$ helix the hydrogen bonding of the ethanolamide OH group occurs with the Gly^2–Ala^3 peptide CO, and the formyl CO remains free (Fig. 19). Hence the presence of a free formamide CO band in the ir spectrum can serve as a test for the presence of a $\uparrow\downarrow\pi\pi^{7.2}_{LD}$ helix. Moreover, in analog (2) the frequency of the main component (1637 cm^{-1}) is higher by 3 cm^{-1} than that for analogs and conformational species of gramicidin A (*7*). At the same time the amide I band of the $\overrightarrow{\pi^{4.4}_{LD}}\overleftarrow{\pi^{4.4}_{LD}}$ and $\overrightarrow{\pi^{6.3}_{LD}}\overleftarrow{\pi^{6.3}_{LD}}$ dimers has a maximum at just about that position (~1650 cm^{-1}, Table 3). By varying the relative contents of the conformational types we were able to obtain an optimal ratio of these types 0.75 $\uparrow\downarrow\pi\pi^{5.6}_{LD}$ + 0.15 $\overrightarrow{\pi^{4.4}_{LD}}\overleftarrow{\pi^{4.4}_{LD}}$ + 0.10 $\overrightarrow{\pi^{6.3}_{LD}}\overleftarrow{\pi^{6.3}_{LD}}$ (Fig. 20b) to give a composite spectrum that would most closely fit the actual spectrum of species 3 (cf. Fig. 20a). A similar fit is obtained with the $\uparrow\downarrow\pi\pi^{7.2}_{LD}$ component instead of the $\uparrow\downarrow\pi\pi^{5.6}_{LD}$ component.

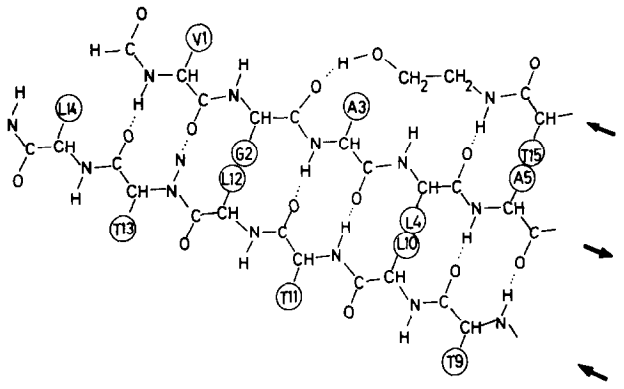

FIG. 19. An unrolled perspective of the $\uparrow\downarrow\pi\pi_{LD}^{1,2}$ helix (the terminal portion of the helix is shown).

The amide I band in the ir spectra calculated for the asymmetric dimers $\overrightarrow{\pi_{LD}^{4,4}}\,\overrightarrow{\pi_{LD}^{4,4}}$ and $\overrightarrow{\pi_{LD}^{6,3}}\,\overrightarrow{\pi_{LD}^{6,3}}$ also has a frequency at 1650 cm^{-1} (Table 3), so that the possible existence of such dimers must be considered. Their presence would entail the presence also of trimers $\overrightarrow{\pi_{LD}}\,\overrightarrow{\pi_{LD}}\,\overrightarrow{\pi_{LD}}$, tetramers, etc. (*7*). Aggregation studies for $N > 2$ showed that in fact such oligomers are absent from the solution. Instead an antiparallel β-structure was found for compound (6), as follows from the characteristic parameters (*25*) of its ir and CD spectra in dioxane at $c \geqslant 10^{-3}\,M$ (Fig. 6). For aggregates with $N > 2$ of analog (3) modeling species 4 similarly to analog (6) there is a considerable decrease in intensity and a shift to longer wavelengths of the entire tryptophan CD spectral band at 228 nm. This indicates that aggregation of $N > 2$ of all the conformers in solution is accompanied by interaction of the tryptophan residues and so is also not the result of a $\overrightarrow{\pi_{LD}}\,\overrightarrow{\pi_{LD}}\,\overrightarrow{\pi_{LD}}$ junction. We, therefore, consider improbable formation of $\overrightarrow{\pi_{LD}}\,\overrightarrow{\pi_{LD}}$ dimers in analogs modeling either species 3 or species 4.

Still another possibility must be considered: the shoulder at 1650 cm^{-1} may be due to an unordered conformation. It was shown in Ref. (*29*) that in DMSO the gramicidin A monomer is unordered. The amide I bands for all the gramicidin A analogs in DMSO ($c < 10^{-2}\,M$) are very broad, ($\Delta\nu_{\frac{1}{2}} = 50$ cm^{-1}) with a maximum at 1660 cm^{-1}, which is close to the spectral parameters of a polypeptide in the random state (*25*). However, since the 1660-cm^{-1} frequency is significantly higher than that of the shoulder (1648 cm^{-1}), the latter cannot be due to disordered structure.

The shoulder at 1648 cm^{-1} present in all the observed ir spectra could also be explained by the presence of the $\uparrow\uparrow\pi\pi_{LD}^{5,6}$ helix in solution in a relative concentration of ca. 25%, because the spectra calculated for this conformation have an intense component at ca. 1650 cm^{-1} (Fig. 14). The synthesis of the amide I band profile for this case is shown in Fig. 20c.

There are thus two possible explanations for the presence of the 1648-cm^{-1} shoulder: the presence in the solution of (i) 25% of π_{LD} helical dimers or of (ii) about the same amount of $\uparrow\uparrow\pi\pi_{LD}^{5,6}$ helical dimer. We believe that actually the first assumption is correct, for the following reasons. As will be clear from the

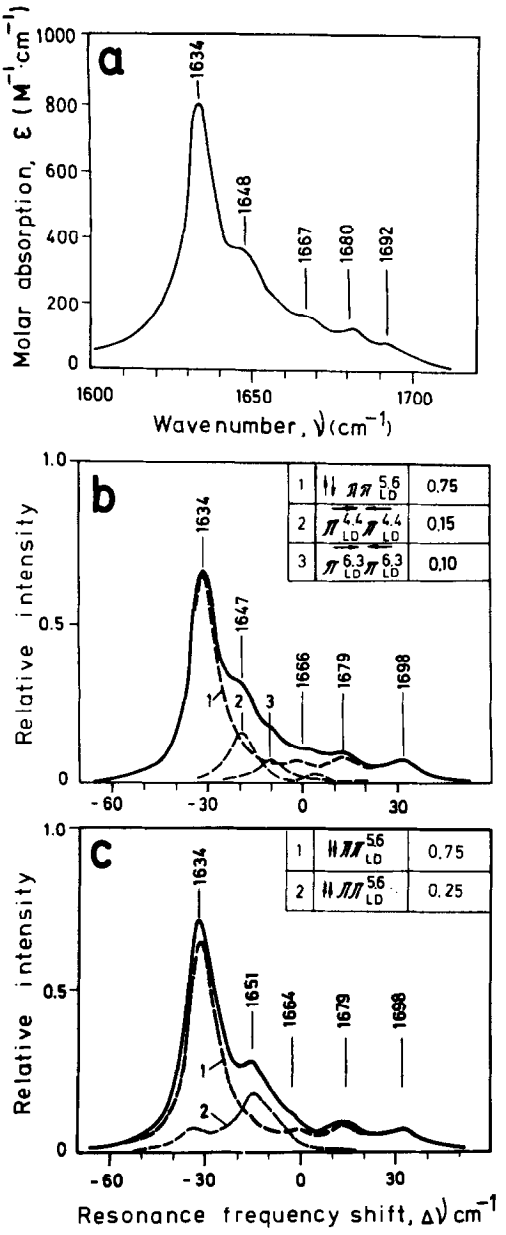

FIG. 20. Comparison of observed and calculated ir spectra of gramicidin A. (a) Observed ir spectrum of gramicidin species 3. (b) Synthesis of the composite amide I band from the spectra of the $\uparrow\downarrow \pi\pi^{5,6}_{LD}$, $\overrightarrow{\pi^{4,4}_{LD}}\,\overleftarrow{\pi^{4,4}_{LD}}$, and $\overrightarrow{\pi^{6,3}_{LD}}\,\overleftarrow{\pi^{6,3}_{LD}}$ models. (c) The same for the $\uparrow\downarrow \pi\pi^{5,6}_{LD}$ and $\uparrow\uparrow \pi\pi^{5,6}_{LD}$ models.

following, monomeric gramicidin A is in the conformation of a $\pi^{4,4}_{LD}$ helix, which makes more natural the presence also of $\overrightarrow{\pi_{LD}}\,\overleftarrow{\pi_{LD}}$ dimers in solution. This assumption is also in agreement with the data of Bamberg *et al.* (*14, 15*) according to which the $\uparrow\uparrow \pi\pi_{LD}$ helix does not occur in gramicidin A embedded in a membrane.

We thus arrive at the conclusion that the ir spectra observed for gramicidin A and its analogs are due to coexistence in solution of three structures, namely ~75% $\Uparrow\Downarrow\pi\pi^{5,6}_{LL}$ (or $\Uparrow\Downarrow\pi\pi^{7,2}_{LL}$), ~15% $\overrightarrow{\pi^{4,4}_{LL}}\overleftarrow{\pi^{4,4}_{LL}}$, and ~10% $\overrightarrow{\pi^{6,3}_{LL}}\overleftarrow{\pi^{6,3}_{LL}}$. This could be realized in two ways: (i) as an equilibrium between the different conformers or (ii) as dimers comprising two π_{LD} helices intertwined to the extent of only 75% (Fig. 21). How-

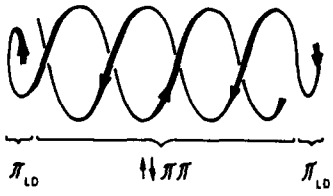

FIG. 21. Schematic presentation of the 0.75 $\Uparrow\Downarrow\pi\pi_{LD}$ + 0.25 π_{LD} "hybrid" dimer.

ever, in the second case the helices should contain nonregular ϕ and ψ angles, especially in the regions of transition from the double- to the single-stranded helix. The presence of such nonregularity would have immediately led to a broadening of the ir bands (*30*). At the same time, we could quite successfully use an additive scheme for the spectra calculated for ideal helices.

In addition, in shortening the chain the number of peptide groups included in a single-stranded π_{LD} helix at the ends of the "hybrid" dimers should diminish. Thus, in the case of analog (7) with $N = 9$ such groups proved to be two at each end, a quantity much too small to account for the presence in the spectrum of the 1650-cm^{-1} band which is present in the spectra of all the analogs, whatever their length. Consequently, the hybrid structure of dimers as shown in Fig. 21 is apparently absent from solutions of gramicidin A or of its analogs.

All these facts lead to the conclusion that each dimeric species is not conformationally homogeneous, but is an equilibrium mixture of three structures of which $\Uparrow\Downarrow\pi\pi^{5,6}_{LD}$ or $\Uparrow\Downarrow\pi\pi^{7,2}_{LD}$ is predominant, whereas $\overrightarrow{\pi^{4,4}_{LD}}\overleftarrow{\pi^{4,4}_{LD}}$ and $\overrightarrow{\pi^{6,3}_{LD}}\overleftarrow{\pi^{6,3}_{LD}}$ are minor.

We have no data that would allow of inferences as to the rates of interconversion of the basic and minor conformations of species 1–4. Inasmuch as, contrary to the species themselves, their conformers are not separated by thin layer chromatography, one naturally supposes that such interconversions are more rapid than between the species. However, one cannot exclude simple coincidence of the R_f values.

As can be seen from Fig. 1 the CD spectra of the dimer species 1, 2, and 3, the gramicidin A monomer and the dimers of their model analogs (2), (4)–(6) in dioxane have negative Cotton effects in the 200- to 250-nm region (Figs. 3, 4). Species 4 and its model analogs (3), (7), (8) give positive Cotton effects in that region (Figs. 4b–d). According to the calculations of Bayley (*31*), a negative effect should be present in the CD spectra (200–230 nm) of the left-handed $\pi^{4,4}_{LD}$ helix, whereas the right-handed α-helix of poly(L-tryptophan) displays an intense positive band at 228 nm (*32*). On this basis we ascribe a left-handed sense to the major components of species 1, 2, and 3 and a right-handed one to the major

TABLE 4

DISSOCIATION RATE OF GRAMICIDIN A DIMERS IN SOLVENTS OF VARYING POLARITY (*8*) AND IN THE MEMBRANE (*5*)

Solvent	K_d (sec^{-1})
Ethyl acetate	$\sim 10^{-6}$
Dioxane	$\sim 10^{-6}$
Ethanol	$\sim 10^{-4}$
Methanol	$\sim 10^{-2}$
Bilayer	~ 1

component of species 4. On passing from the dimer to the $\pi_{LD}^{4,4}$ helical monomer (see below) the sign of the Cotton effect including that of the 228-nm band is retained in the spectra of both gramicidin A and of its analogs (Figs. 2–4). Since the minor components are addends of the π_{LD} monomer, to them too can be ascribed the same helicity. This means that all helices, both dimeric and monomeric, belonging to species 4 are right handed, whereas for species 1 + 2 and 3, they are left handed (Table 5).

In the case of gramicidin A and its analogs with $N \geq 13$, not only the sign but also the entire CD spectrum (200–250 nm) is retained on passing from the dimer to the monomer. Consequently tryptophan is in the same conformation in the monomer as in the dimer, and we see that in the interconversions of the forms within each species (shown in the final equilibrium Eq. [3], see below) not only the direction of rotation of the helices, but the conformations of the Trp residues are retained.

In Ref. (*33*) the energetically favorable rotatory angles χ^1 and χ^2 of the Trp residues for the right-handed gramicidin A $\pi_{LD}^{4,4}$ and $\pi_{LD}^{6,3}$ helices were found to be 180 and 90°, 180 and −90°, −60 and 90°, respectively. The −60°, −90° conformation cannot be realized in right-handed $\pi_{LD}^{4,4}$ helices. Retention of the conformations of Trp in equilibrium Eq. [3], therefore, means that this conformation cannot correspond to species 4. The angles indicated can occur in several, but quite

TABLE 5

CONFORMATIONS OF GRAMICIDIN A IN DIOXANE SOLUTION

Species	Helicity	Type of helices and their mole fractions
1	Left handed	$0.75 \; \uparrow\downarrow \pi\pi_{LD}^{1,2} + 0.15 \; \overrightarrow{\pi_{LD}^{4,4}} \; \overleftarrow{\pi_{LD}^{4,4}} + 0.10 \; \overrightarrow{\pi_{LD}^{6,3}} \; \overleftarrow{\pi_{LD}^{6,3}}$
2	Left handed	$0.75 \; \uparrow\downarrow \pi\pi_{LD}^{1,2} + 0.15 \; \overrightarrow{\pi_{LD}^{4,4}} \; \overleftarrow{\pi_{LD}^{4,4}} + 0.10 \; \overrightarrow{\pi_{LD}^{6,3}} \; \overleftarrow{\pi_{LD}^{6,3}}$
3	Left handed	$0.75 \; \uparrow\downarrow \pi\pi_{LD}^{3,6} + 0.15 \; \overrightarrow{\pi_{LD}^{4,4}} \; \overleftarrow{\pi_{LD}^{4,4}} + 0.10 \; \overrightarrow{\pi_{LD}^{6,3}} \; \overleftarrow{\pi_{LD}^{6,3}}$
4	Right handed	$0.75 \; \uparrow\downarrow \pi\pi_{LD}^{3,6} + 0.15 \; \overrightarrow{\pi_{LD}^{4,4}} \; \overleftarrow{\pi_{LD}^{4,4}} + 0.10 \; \overrightarrow{\pi_{LD}^{6,3}} \; \overleftarrow{\pi_{LD}^{6,3}}$

definite orientations of the D-Leu side chains. A corresponding set of favorable χ^1 and χ^2 angles should occur also in the left-handed helices. One could also expect that in the double helices no additional allowed structures would be present in the case of Trp, but that, on the contrary, more constraints could arise. An examination of CPK models has shown that in the $\uparrow\downarrow\pi\pi^{7,2}_{LD}$ helix such constraints are absent but that in the left-handed $\uparrow\downarrow\pi\pi^{5,6}_{LD}$ helix (the basic conformation of species 3) the 180°, 90° parameters are hindered. Further refinement of the χ^1 and χ^2 angles of species 1–4 would be premature. However, we believe that the structural differences in species 1 and 2 are due just to differences in the χ^1 and χ^2 angles of the tryptophan side chains.

Transitions except for $1 \rightleftarrows 2$ between the various species are thus associated with conformational rearrangement of both the backbone ($\uparrow\downarrow\pi\pi_{LD}$ helices) and of the Trp residues. Most likely the energy minimum of the $\uparrow\downarrow\pi\pi_{LD}$ helices of the different species (Table 5) is achieved by coordinated conformational changes in the backbone and in the Trp residues. It is to be noted that for interconversion of the right-handed and left-handed $\uparrow\downarrow\pi\pi^{5,6}_{LD}$ helices ($3 \rightleftarrows 4$) (Table 5) and of the $\uparrow\downarrow\pi\pi^{7,2}_{LD}$ and $\uparrow\downarrow\pi\pi^{5,6}_{LD}$ helices of the same sign ($2 \rightleftarrows 3$ and $1 \rightleftarrows 3$), only half the hydrogen bonds have to be ruptured (14 out of 28), since the intermediate state of these transitions is the $\uparrow\downarrow$ β-structure. The transition $1 \rightleftarrows 2$ is only a change in orientation of the indole radicals; hence it becomes clear why it is more rapid than equilibration with participation of the other species (*8*).

Let us consider the monomeric state of gramicidin A and its analogs. From a comparison of the CD spectra (200–250 nm) of the gramicidin A analogs it can be seen that the amplitudes of the curves for the greatly shortened monomer analogs (6)–(8) (Figs. 4a,b,d) with $N \precsim 11$ are much lower than those for the dimers, whereas for analogs with $N \succsim 13$ (2–5) (Figs. 3, 4c) this difference is small. In ethanol the monomer and dimer spectra differ for all the analogs (see, for example Fig. 5).

The diminished amplitude of the CD spectra in ethanol is explained by dilution-induced rearrangement of the dimer helical conformations to an unordered structure characteristic of nonregular polypeptides in polar media. In dioxane the results show that with greatly shortened analogs ($N \precsim 11$) the monomer may have a random structure, whereas long analogs have an ordered helical structure, even for the monomer.

What then is the conformation of the gramicidin A monomer? In the monomeric state gramicidin A and analog (3), ($N = 15$) have an amide I band frequency of 1650 cm^{-1}, whereas analogs (5)–(7) have a frequency of 1653 cm^{-1} (Figs. 11, 12). In the case of analog (5) it was possible to obtain the spectrum for the "pure" monomer (Fig. 11). The spectra calculated for the $\pi^{4,4}_{LD}$ helical monomer of the corresponding length gave quite close frequencies 1654 cm^{-1} ($N = 15$) and 1656 cm^{-1} ($N = 13$) (Table 3), whereas the spectra of the $\pi^{6,3}_{LD}$ helical monomer would have had much higher frequencies (1663–1670) (Table 3). It is noteworthy that the half-widths of the calculated and experimental bands for the $\pi^{4,4}_{LD}$ helix of the monomer are also close in value (16 and 12 cm^{-1}, respectively). The resultant data show that in nonpolar solvents the monomeric gramicidin A backbone has only a single conformation (if the possibility of opposite handedness of the helix be

disregarded), and that it is the conformation of a $\pi_{LD}^{4,4}$ helix. Interestingly, a length of 13 residues (~three turns) is sufficient for a stable helix. According to the ir data, in the monomeric state analog (8) ($N = 9$) has a high content of unordered structure, i.e., a length of two turns may be insufficient for stabilizing the $\pi_{LD}^{4,4}$ helix of a nonregular peptide in a nonpolar media. An intermediate position is assumed by analogs (7) and (6) ($N = 11$). The ir data show that in the monomeric state they are in the form of a $\pi_{LD}^{4,4}$ helix, whereas in the CD spectrum we observed considerable diminution of band intensity relative to the dimers. Apparently this is due to the fact that whereas in the monomer the backbond preserves its conformation, the side chains, in particular the side chains of the Trp residues, acquire rotational freedom.

It follows from the above that the solution conformational equilibrium of any of the species 1–4 can be depicted in the following manner:

$$\begin{array}{c} \Uparrow\Downarrow\pi\pi_{LD}^{5,6}\ (\text{or}\ \Uparrow\Downarrow\pi\pi_{LD}^{7,2}) \rightleftarrows \overrightarrow{\pi_{LD}^{4,4}}\,\overleftarrow{\pi_{LD}^{4,4}} + \overrightarrow{\pi_{LD}^{6,3}}\,\overleftarrow{\pi_{LD}^{6,3}} \\ \searrow\!\swarrow\ \pi_{LD}^{4,4}\ \searrow\!\swarrow \end{array} \qquad [3]$$

Since the dimer–monomer transition in nonpolar solvent is slow for all species (*8*) (Table 4), interconversion of the dimeric forms should take place without monomer participation, for instance by way of the "zipper" mechanism proposed by Urry (*22*). According to this mechanism the $\Uparrow\Downarrow\pi\pi_{LD}$ helices are completely intertwined π_{LD} helices, and their association (formation of the $\overrightarrow{\pi_{LD}}\,\overleftarrow{\pi_{LD}}$ dimer) is the first step in this involution. Such type of transition requires retention of the helical sense.

In polar solvents the dissociation rate of the dimer greatly increases (Table 4), and equilibration between the $\overrightarrow{\pi_{LD}}\,\overleftarrow{\pi_{LD}}$ dimers and the $\Uparrow\Downarrow\pi\pi_{LD}$ helix can take place through both the monomer and the "zipper" mechanism, i.e., the entire Eq. [3] is realized. The data of Glickson *et al.* (*34*) on H–D exchange in gramicidin A in a polar solvent (DMSO) and their interpretation are neither in disagreement with the "monomer" nor with the "zipper" equilibration mechanisms.

Factors Determining Dimer Stability

According to Veatch and Blout (*8*), who measured the dissociation of dimeric gramicidin A in a 4 : 1 ethyl acetate : ethanol mixture by PF, the process takes 8 hr for species 3 and 40 hr for species 4. We carried out an independent determination by ir spectroscopy of the half-times for transition of gramicidin A species 3 in dioxane from 100% dimer to 50% dimer : 50% monomer (Table 2). Since the absorption frequencies of the helical monomer and the $\overrightarrow{\pi_{LD}^{4,4}}\,\overleftarrow{\pi_{LD}^{4,4}}$ and $\overrightarrow{\pi_{LD}^{6,3}}\,\overleftarrow{\pi_{LD}^{6,3}}$ dimers are close to each other (1654, 1647, and 1656 cm^{-1}, respectively, Table 3) we have actually determined the dissociation time of only the $\Uparrow\Downarrow\pi\pi_{LD}$ helical conformer, but we can say nothing about the dissociation rate of the $\overrightarrow{\pi_{LD}}\,\overleftarrow{\pi_{LD}}$ dimers. In measuring the dissociation rate of the gramicidin A dimer by PF (*8*), rapid dissociation of a conformer of the same thermodynamic stability as the slowly dissociating one could also have escaped observation.

Our data confirm the fact that in a nonpolar medium, transition of the gramicidin A dimer to monomer is a very slow process (Table 2). Comparison of the

transition half-times given in this table shows that on shortening the chain to N = 11 the dimer dissociation rate of species 3 (analog 6) and species 4 (analog 7) increases about a 100-fold. This is natural for the unraveling of a double helix, the time for which should diminish with diminution of the number of its turns. At the same time, the dimerization eqiilibrium constants of these analogs remains the same as for gramicidin A (Table 1); hence with shortening of the chain (down to N = 11) the 100-fold increase in rate pertains not only to unraveling of the double helix, but to its formation. Since, however, the dissociation rate of analogs (5) (N = 13) and (6) (N = 11) are practically the same, this means that the rate of dimer dissociation depends not only on the chain length, but also on the amino acid sequence, i.e., on the steric interactions of the side chains.

Retention of the high K_{dim} equilibrium constants in analogs (7) and (6) in dioxane (Table 1) shows that for a $\uparrow\downarrow \pi\pi^{5,6}_{LD}$ helix (the predominant conformation of these analogs) two turns for each chain are sufficient for stabilization of the structure in nonpolar medium.

In compound (1) the glycine residue in position 9 divides the chain into two portions, each of which has altering LD residues. The low CD amplitudes, the broadening and low intensity of the amide I band ($\Delta\nu_{\frac{1}{2}}$ = 50 cm^{-1}, ϵ = 280 $M^{-1} \cdot cm^{-1}$), and the appearance of a 1534-cm^{-1} component in the amide II band bear evidence of the absence of ordered structures (*25*). On the other hand, the low dimerization constants of analog (1) also demonstrate the inadequacy of 1.2–1.4 turns (7–8 residues in each chain) to stabilize a double helix.

The thermodynamic stability of dimers depends not only on the length of the backbone, but also on the nonbonded interactions of the side chains, i.e., on the sequence of the amino acids, as evidenced by diminution of K_{dim} of analogs (2), (4), (5) to 10^2–10^3 M^{-1} (Table 1).

Relationship between the Gramicidin A Solution Conformations and the Structure of the Transmembrane Channel

The present investigation of gramicidin A and its analogs has been carried out mainly on substances in a nonpolar solvent (dioxane) which can serve as a model of a membrane environment. One may conclude on these grounds that in general the same conformational equilibrium (Eq. [3]) exists in the membrane as in a nonpolar solvent. However, here, interconversion of the former must proceed *via* the monomer, as dissociation of the dimer in the membrane is much faster than in a nonpolar solvent (Table 4), a fact that explains the short lifetime of a gramicidin A channel (~1 sec). A priori one cannot exclude the possibility of the conformational interconversions in the membrane occurring by the "zipper" mechanism shown in the upper line of Eq. [3], wherein the overall length of the dimer is retained and the functioning of the channel is uninterrupted, only a change in its conductivity taking place. However, as one can see from the conductivity data of individual gramicidin A channels (*5, 14*) conductivity changes occur only through formation of nonconducting states, most likely via the monomer (*5*). Consequently in the membrane the equilibrium

$$\Uparrow\Downarrow \pi\pi^{5,6}_{LD} \text{ (or } \Uparrow\Downarrow \pi\pi^{7,2}_{LD}) \rightleftarrows \pi^{4,4}_{LD} \rightleftarrows \overrightarrow{\pi_{LD}}\,\overleftarrow{\pi_{LD}} \qquad [4]$$

takes place.

There is a striking increase (by 6 orders of magnitude) of the dimer dissociation rate in the membrane as compared with the nonpolar solvent. Table 2 shows that the transition from the gramicidin A double helix ($N = 15$, ~2.7 turns per chain) to shorter helices ($N = 11$, ~2 turns per chain) increases the dissociation rate by about 2 orders of magnitude. One might, therefore, assume that the rate increase of gramicidin A dissociation in the membrane could be due to a shift in the conformational equilibrium (Eq. [4]) from a predominant (75%) $\Uparrow\Downarrow \pi\pi_{LD}$ helix in solution to the Urry $\overrightarrow{\pi_{LD}}\,\overleftarrow{\pi_{LD}}$ dimer, which can dissociate merely by one turn of the π_{LD} helix with respect to the other about their common axis.

As seen in Table 2 the double helix dissociation times are greatly dependent on chain length and the amino acid sequence. A study of analogs (3–5) on an egg lecithin bilayer (*35*) showed that all these analogs have channel lifetimes within the range of 0.8–5 sec, i.e., of the same order of magnitude as the gramicidin A channels (*5, 14*). The absence of relationships between the helical dimer lifetimes of different analogs in dioxane and of the membrane channel lifetimes of these analogs confirms the assumption of the predominance of $\overrightarrow{\pi_{LD}}\,\overleftarrow{\pi_{LD}}$ dimers in the membrane. This is in accord with the data of Bamberg *et al.* (*14*), who showed that head-to-head covalently bonded malonyl-bis-desformylgramicidin can form a membrane channel. In this light, of interest are the results concerning *N*-acetyl-desformyl gramicidin A, where the formation of $\overrightarrow{\pi_{LD}}\,\overleftarrow{\pi_{LD}}$ dimers but not of double helices is sterically hindered. According to Gooddall (*36*) this analog is much less active than gramicidin A on a lipid bilayer. On the other hand Veatch and Blout (*8*) found that substitution of a formyl proton by a methyl group affects significantly neither K_{dim} nor the relative species content. This discrepancy can be explained if it is assumed that there is a shift in equilibrium (Eq. [4]) from the $\Uparrow\Downarrow \pi\pi_{LD}$ helix in solution to the Urry dimer in the membrane.

The existence of two different conformers in $\overrightarrow{\pi_{LD}}\,\overleftarrow{\pi_{LD}}$ helices of gramicidin A in solution is evidence of the energetic similarity of these two forms. Therefore, in the passage of an ion through a gramicidin A channel, local, reversible conformational transitions can occur, thus providing for the best fit of the internal channel diameter to the size of the ion. The internal diameter of a $\pi^{4,4}_{LD}$ helix (~1.4 Å) is insufficient for the passage of even sodium, so that for this to occur one must assume that in the helices local rearrangements: $\pi^{4,4}_{LD}$ (without ion) $\rightleftarrows$ $\pi^{6,3}_{LD}$ (with ion) occur, which are propagated along the gramicidin A channel concurrently with the moving ion. Chandler et al. (*37*) considered such conformational changes in the α-helical polypeptide chains as gliding edge dislocations, assuming that α–π type transitions could provide for translocation of Na^+ and Ca^{2+} ions along the helical pore. They proposed that such a mechanism is operative in Na- and Ca-ATPases. A finer adaptation of the $\pi^{6,3}_{LD}$ helix to the cation diameter can take place by deviation of the peptide planes from their equilibrium positions, in which they are parallel to the helical axis. Such conformational changes could pucker the ion containing part of the helix at the expense of narrowing the inner cavity of the other part.

Conclusion

The results of the present study force a reassessment of the accepted notions on the nature of the conformational equilibrium of gramicidin A. Indeed, in the references cited, the implicit inference had been made that each of the four dimeric gramicidin A species is conformationally homogeneous (at least with respect to the backbone structure) and that the problem consisted in ascribing to these species a given helix type. Actually the situation is more complicated: namely, each of the four "species" is itself an equilibrium mixture of a number of helical forms, although in all cases the $\uparrow\downarrow \pi\pi_{LD}$ helix is predominant.

Noteworthy also is that the $\overrightarrow{\pi_{LD}}\overleftarrow{\pi_{LD}}$ dimer, which on all grounds seems to be the one whereby gramicidin A carries out its channel function, turned out to be a minor form in nonpolar solution. Apparently, we are dealing here with the rare case of considerable conformational change accompanying passage from a nonpolar solvent to the lipid zone of a membrane.

Finally, it should be remembered that there are as yet no direct indications that the functional role of gramicidin A in the metabolism of its producer organism is induction of membrane ion permeability. On the contrary, the existing facts favor the mechanism whereby the primary act of gramicidin A is inhibition of RNA polymerase with subsequent development of sporulation (*38*). It cannot be excluded that here the operational structure of the antibiotic is that of a double helix.

ACKNOWLEDGMENTS

We would like to express our thanks and appreciation to Professor Yu. A. Ovchinnikov and Dr. Yu. N. Chirgadze for their interest and valuable advice.

REFERENCES

1. J. B. CHAPPELL AND A. R. CROFTS, *Biochem. J.* **95,** 393 (1965).
2. S. B. HLADKY AND D. A. HAYDON, *Nature (London)* **225,** 451 (1970).
3. D. C. TOSTESON, T. E. ANDREOLI, M. TIEFFERBERG, AND P. COOK, *J. Gen. Physiol.* **51,** 373S (1968).
4. E. BAMBERG AND P. LÄUGER, *Biochim. Biophys. Acta* **367,** 127 (1974).
5. W. R. VEATCH, R. MATHIES, M. EISENBERG, AND L. STRYER, *J. Mol. Biol.* **99,** 75 (1975).
6. W. VEATCH AND L. STRYER, *J. Mol. Biol.* **113,** 89 (1977).
7. W. R. VEATCH, E. T. FOSSEL, AND E. R. BLOUT, *Biochemistry* **13,** 5249 (1974).
8. W. R. VEATCH AND E. R. BLOUT, *Biochemistry* **13,** 5256 (1974).
9. G. N. RAMACHANDRAN AND R. CHANDRASEKARAN, "Progress in Peptide Research," (S. Lande, Ed.), pp. 195–215. Gordon & Breach, New York/London/Paris, 1972; see also *Indian J. Biochem. Biophys.* **9,** 1 (1972).
10. D. W. URRY, *Proc. Natl. Acad. Sci. USA* **68,** 672 (1971).
11. D. W. URRY, M. C. GOODALL, J. D. GLICKSON, AND D. F. MAYERS, *Proc. Nat. Acad. Sci. USA* **68,** 1907 (1971).
12. F. HEITZ, B. LOTZ, AND G. SPACH, *J. Mol. Biol.* **92,** 1 (1975).
13. B. LOTZ, F. COLLONNA-CESARI, F. HEITZ, AND G. SPACH, *J. Mol. Biol.* **106,** 915 (1976).
14. E. BAMBERG AND K. JANKO, *Biochim. Biophys. Acta* **465,** 486 (1977).

15. H. J. APELL, E. BAMBERG, H. ALPES, AND P. LÄUGER, *J. Membrane Biol.* **31,** 171 (1977).
16. E. BAMBERG, H. J. APELL, AND H. ALPES, *Proc. Nat. Acad. Sci. USA* **74,** 2402 (1977); E. BAMBERG, H. J. APELL, H. ALPES, E. GROSS, J. L. MORELL, J. F. HARBAUGH, K. JANKO, AND P. LÄUGER, *Fed. Proc.* **12,** 2633 (1978).
17. R. J. BRADLEY, D. W. URRY, K. OKAMOTO, AND R. RAPAKA, *Science* **200,** 435 (1978).
18. E. N. SHEPEL, ST. JIORDANOV, I. D. RYABOVA, A. I. MIROSHNIKOV, V. T. IVANOV, AND YU. A. OVCHINNIKOV, *Bioorg. Chem. (USSR)* **2,** 581 (1976).
19. YU. N. CHIRGADZE AND N. A. NEVSKAYA, *Biopolymers* **15,** 607 (1976).
20. YU. N. CHIRGADZE AND N. NEVSKAYA, *Biopolymers* **15,** 627 (1976).
21. N. A. NEVSKAYA AND YU. N. CHIRGADZE, *Biopolymers* **15,** 637 (1976).
22. D. W. URRY, M. M. LONG, M. JACOBS, AND R. D. HARRIS, *Ann. N.Y. Acad. Sci.* **264,** 203 (1975).
23. W. A. VEATCH, "Gramicidin A—Conformation and Aggregation," Ph.D. Thesis, p. J-28. Harvard University, Cambridge, Mass., 1973.
24. L. J. BELLAMY, "The Infra-Red Spectra of Complex Molecules," 3rd ed., p. 238. Chapman & Hall, London, 1975.
25. YU. N. CHIRGADZE, B. V. SHESTOPALOV, AND S. YU. VENYAMINOV, *Biopolymers* **12,** 1337 (1973).
26. T. MIYAZAWA, *J. Chem. Phys.* **32,** 1647 (1960).
27. F. COLLONNA-CESARI, S. PREMILAT, F. HEITZ, G. SPACH, AND B. LOTZ, *Macromolecules* **10,** 1284 (1977).
28. R. E. KOEPPE II, K. O. HODGSON, AND L. STRYER, *J. Mol. Biol.* **121,** 41 (1978).
29. E. T. FOSSEL, W. R. VEATCH, YU. A. OVCHINNIKOV, AND E. R. BLOUT, *Biochemistry* **13,** 5264 (1974).
30. YU. N. CHIRGADZE, E. V. BRAZHNIKOV, AND N. A. NEVSKAYA, *J. Mol. Biol.* **102,** 781 (1976).
31. P. M. BAYLEY, *Progr. Biophys. Mol Biol.* **27,** 58 (1973).
32. E. PEGGION, A. COSANI, A. S. VERDINI, A. DEL PRA, AND M. MAMMI, *Biopolymers* **6,** 1477 (1968).
33. E. M. POPOV AND G. M. LIPKIND, *Mol. Biol. (USSR)* **13,** 363 (1979).
34. J. D. GLICKSON, D. F. MAYERS, J. M. SETTINE, AND D. W. URRY, *Biochemistry* **11,** 477 (1972).
35. YU. A. OVCHINNIKOV AND V. T. IVANOV, "Biochemistry of Membrane Transport" (G. Semenza and E. Carafoli, Eds.), FEBS-Symposium No. 42, pp. 123–146. Springer-Verlag, Berlin/Heidelberg/New York, 1977.
36. M. C. GOODALL, *Arch. Biochem. Biophys.* **147,** 129 (1971).
37. H. D. CHANDLER, C. J. WOOLF, AND H. R. HEPBURN, *Biochem. J.* **169,** 559 (1978).
38. N. SARKAR, D. LANGLEY, AND H. PAULUS, *Proc. Nat. Acad. Sci. USA* **74,** 1478 (1977).